JOURNAL OF VIROLOGY, Sept. 2008, p. 8560–8569 Vol. 82, No. 17
0022-538X/08/$08.00+0 doi:10.1128/JVI.00699-08

T Lymphocytes Contribute to Antiviral Immunity and Pathogenesis in Experimental Human Metapneumovirus Infection▽

Deepthi Kolli,[1]† Efthalia L. Bataki,[1]† LeAnne Spetch,[1] Antonieta Guerrero-Plata,[1] Alan M. Jewell,[4] Pedro A. Piedra,[4] Gregg N. Milligan,[1,2,3] Roberto P. Garofalo,[1,2,3] and Antonella Casola[1,2,3]*

Departments of Pediatrics[1] and Microbiology and Immunology[2] and Sealy Center for Vaccine Development,[3] University of Texas Medical Branch, Galveston, and Department of Molecular Virology and Microbiology, Baylor College of Medicine, Houston,[4] Texas

Received 28 March 2008/Accepted 10 June 2008

Human metapneumovirus (hMPV), a member of the family *Paramyxoviridae*, is a leading cause of lower respiratory tract infections in children, the elderly, and immunocompromised patients. Virus- and host-specific mechanisms of pathogenesis and immune protection are not fully understood. By an intranasal inoculation model, we show that hMPV-infected BALB/c mice developed clinical disease, including airway obstruction and hyperresponsiveness (AHR), along with histopathologic evidence of lung inflammation and viral replication. hMPV infection protected mice against subsequent viral challenge, as demonstrated by undetectable viral titers, lack of body weight loss, and a significant reduction in the level of lung inflammation. No cross-protection with other paramyxoviruses, such as respiratory syncytial virus, was observed. T-lymphocyte depletion studies showed that $CD4^+$ and $CD8^+$ T cells cooperate synergistically in hMPV eradication during primary infection, but $CD4^+$ more than $CD8^+$ T cells also enhanced clinical disease and lung pathology. Concurrent depletion of $CD4^+$ and $CD8^+$ T cells completely blocked airway obstruction as well as AHR. Despite impaired generation of neutralizing anti-hMPV antibodies in the absence of $CD4^+$ T cells, mice had undetectable viral replication after hMPV challenge and were protected from clinical disease, suggesting that protection can be provided by an intact $CD8^+$ T-cell compartment. Whether these findings have implications for naturally acquired human infections remains to be determined.

Human metapneumovirus (hMPV) is a recently identified human respiratory viral pathogen belonging to the family *Paramyxoviridae*, which includes two subfamilies, the *Paramyxovirinae* and the *Pneumovirinae*. The *Pneumovirinae* are taxonomically divided into the *Pneumovirus* and *Metapneumovirus* genera, based primarily on their gene constellations. Respiratory syncytial virus (RSV), an important cause of pediatric respiratory illness, belongs to the *Pneumovirus* genus, while hMPV has been assigned to the *Metapneumovirus* genus, based on genomic sequence analysis (29). Metapneumoviruses lack the nonstructural proteins NS1 and NS2, and the gene order is different from that of pneumoviruses. hMPV is the first human virus of this group; the only other member is the avian pneumovirus, an etiological agent of respiratory infections in turkeys. Since the discovery of hMPV in The Netherlands (30), the virus has been identified in many different countries, including Australia (24), Canada (3), the United Kingdom (28), Finland (28), France (9), South America, and the United States (7, 8, 32). hMPV has a seasonal distribution (it is usually isolated during the winter) and is associated with both upper and lower respiratory tract infections in children and adults (7, 8, 32). A number of children with proven hMPV infections have a clinical syndrome consistent with bronchiolitis: they present with wheezing, hypoxia, and other typical radiological findings (7, 18, 32). According to different reports, 5 to 12% of all respiratory tract infections in younger infants are caused by hMPV, a proportion second only to that of RSV. hMPV is also responsible for 10% of all hospitalizations of elderly patients with respiratory tract infections (7, 8, 32).

The pathophysiology of hMPV infection and the possible contribution of the host immune response to the pathogenesis of hMPV-induced lower airway disease are largely unknown. In particular, whether T lymphocytes may be involved in antiviral immunity against hMPV, as well as contributing to lung disease, is not fully understood. Studies of experimental RSV infection in mice have shown that the T-cell response helps to resolve RSV infection but also contributes to the pathogenesis of disease. In particular, depletion of $CD4^+$ or $CD8^+$ T cells reduced disease, and depletion of both subsets resulted in long-term infection without clinical illness (11).

Experimental animal models of hMPV infection have been reported, including primates and rodents (1, 14, 22, 33, 34). BALB/c mice have been shown to be permissive to hMPV replication (1, 14). Therefore, in this study, we used an experimental BALB/c mouse model to determine the roles of T-lymphocyte subsets in immunity against primary and secondary hMPV infection in mice as well as their contributions to clinical illness, pulmonary inflammation, airway obstruction, and airway hyperresponsiveness (AHR).

MATERIALS AND METHODS

Viral preparation and titer. The hMPV strain CAN97-83 was obtained from the Centers for Disease Control and Prevention, Atlanta, GA, with permission from Guy Boivin. Virus was propagated in LLC-MK2 cells in minimal essential medium (without serum) containing 1.0 μg trypsin/ml (crude virus). To increase the viral titer for infection, filtered hMPV was prepared using Millipore filters

* Corresponding author. Mailing address: Department of Pediatrics, 301 University Blvd., Galveston, TX 77555-0366. Phone: (409) 747-0581. Fax: (409) 772-1761. E-mail: ancasola@utmb.edu.

† D.K. and E.L.B. contributed equally to this work.

▽ Published ahead of print on 18 June 2008.

with a 100,000 molecular weight cutoff. Viral and cellular preparations were routinely tested for mycoplasma contamination by PCR and were used if they had <0.125 endotoxin unit/ml (by a *Limulus* assay). Viral titers were determined by a 50% tissue culture infective dose ($TCID_{50}$) assay. A 48-well plate of confluent LLC-MK2 cells was infected with serial 1/3 dilutions of the virus in a total volume of 250 μl of medium without serum. The plate was incubated overnight in a humidified incubator (37°C, 5% CO_2), and on the next day the inoculum was removed, and cells were washed with serum-free medium and observed for signs of cytopathic effect (CPE) between 7 and 14 days. The dilution at which 50% CPE was observed was determined to be the $TCID_{50}$ for the virus. For titration of viruses isolated from the lungs of mice, mice were sacrificed on days 1, 2, 3, 5, 7, 9, 14, and 21, the thoracic cavity was opened, and the heart and lungs were removed en bloc. After blood was rinsed through the right ventricle, the lungs were separated from the heart, weighed, and homogenized in minimal essential medium in a 10% (wt/vol) ratio. Homogenized samples were centrifuged, and viral titers in supernatants were determined using serial twofold dilutions.

Mouse infection protocol. Six- to 7-week-old female BALB/c mice (Harlan, Houston, TX) were inoculated intranasally (i.n.) with 10^7 $TCID_{50}$s of filtered hMPV in a total volume of 100 μl. Control mice were inoculated with the same volume of virus-free medium (referred to herein as mock infection). At the indicated time points after infection, lungs were isolated and processed for viral titration and histopathological studies (12). Bronchoalveolar lavage (BAL) was performed to determine total-cell counts and counts of different types of cells as described elsewhere (12).

Flow cytometry of lung cells. For flow cytometry analysis, lungs were collected and digested with collagenase, and cells were passed through nylon mesh. Cells were incubated with an Fc block (anti-mouse CD16/CD32) to reduce nonspecific binding for 30 min before the addition of antibodies (BD Pharmingen) against surface markers: anti-CD3ε, anti-CD4, anti-CD8β, and anti-CD25 for T cells, and anti-Ly6G and anti-Ly6C (Gr-1) for neutrophils. Relevant isotype control antibodies were used throughout. Data were analyzed using FlowJo software (Tree Star).

Depletion of T lymphocytes. Mice were treated with 240 μg of an anti-CD8 antibody (clone 2.43; a generous gift of S. Peebles, Vanderbilt University), 150 μg of anti-CD4 (clone GK1.5), or 240 μg of control immunoglobulin G (IgG). In the acute depletion protocol (protocol 1), antibodies were given intraperitoneally (i.p.) on three consecutive days before infection and also on day 1 postinfection. In the chronic depletion protocol (protocol 2), antibodies were given on three consecutive days before infection and at days 1, 7, 14, 21, and 28 postinfection. Both these treatment protocols have been shown to be effective in depleting more than 90% of both $CD4^+$ and $CD8^+$ T-cells (11, 23).

Clinical disease. The severity of illness in mice was scored daily by two investigators using a standardized 0-to-5 grading system (12). In addition, daily determination of body weight was used to monitor the progression of disease over the experimental period.

Lung histopathology. Lungs were perfused, fixed in 10% buffered formalin, and embedded in paraffin. Multiple 4-μm-thick sections were stained with hematoxylin and eosin (H&E) (5, 12). Briefly, inflammatory infiltrates were scored by enumerating the layers of inflammatory cells surrounding the vessels and bronchioles. Zero to three layers of inflammatory cells were considered "normal." Moderate to abundant infiltrates (>3 layers of inflammatory cells surrounding 50% or more of the circumference of the vessel or bronchioles) were considered "abnormal." The number of abnormal perivascular and peribronchial spaces divided by the total perivascular and peribronchial spaces is the percentage reported as the pathology score. A total of ~15 perivascular and peribronchial spaces per lung were counted for each animal. Slides were analyzed and scored for cellular inflammation under light microscopy in a blinded manner by a trained pathologist. Lung sections were also stained with periodic acid-Schiff stain (PAS) to identify mucus-producing cells.

Microneutralization assay for measurement of serum anti-hMPV antibodies. Heat-inactivated sera were tested for neutralizing antibodies to hMPV as previously described (34). The neutralizing antibody titers were defined as the $\log_2$ of the reciprocal of the highest serum dilution at which a ≥50% reduction in CPE was observed. The lowest detectable titer was 2.5 $\log_2$. Samples with undetectable titers were assigned a value of 2 $\log_2$.

AHR. AHR was assessed in unrestrained mice using whole-body barometric plethysmography (Buxco, Troy, NY) to record enhanced pause (Penh), as previously described (5). Penh is a dimensionless value that represents a function of the ratio of peak expiratory flow to peak inspiratory flow and a function of the timing of expiration. Penh has previously been validated in animal models of AHR (13, 15, 16, 27) and infection-associated airway obstruction (31). Respiratory activity was recorded for 4 min in order to establish baseline Penh values. Mice were subsequently exposed to increasing doses of nebulized methacholine (3, 12, 25, and 50 mg/ml) for 1.5 min, and data were recorded for another 3 min.

Respiratory mechanics. Invasive analysis of lung function was performed on anesthetized mice using the Flexivent system (Scireq, Montreal, Quebec, Canada), which integrates a computer-controlled small-animal ventilator with measurements of respiratory mechanics (4). Mice were anesthetized with xylazine (7 mg/kg) and pentobarbital sodium (50 mg/kg of body weight), and the tracheae were cannulated with an 18G tubing adaptor for the delivery of methacholine. Mice were artificially ventilated at 150 breaths/min with a tidal volume of 0.3 ml and a positive end expiratory pressure of 3 cm H_2O. Mice were allowed to stabilize on the ventilator for 5 min before measurements commenced. Measurements of baseline pulmonary mechanics and responses to aerosolized methacholine (0 to 50 mg/ml saline; delivered by ultrasonic nebulizer) were then obtained by using the forced-oscillation technique (19). Aerosols were delivered for 10 s without altering the ventilatory pattern, after which the 8-s forced-oscillation perturbation was applied every 30 s for 5 min. Peak responses during each 5-min period were determined for resistance. Responsiveness to methacholine was assessed at 5, 8, and 14 days post-hMPV infection for four mice per group.

Statistical analysis. When two groups were compared, the values were analyzed using an unpaired, two-tailed Student *t* test. When multiple groups were compared, analysis of variance was used (GraphPad Instat Software, Inc., San Diego, CA). The inflammation scores were analyzed using SAS. Results are expressed as means ± standard errors of the means (SEM) unless otherwise stated.

RESULTS

hMPV-induced clinical disease and viral replication in the lung. BALB/c mice were inoculated i.n. with either hMPV, UV-inactivated hMPV, or mock medium. Following an initial phase (days 1 to 3) with modest body weight loss and rapid recovery, hMPV-infected mice consistently showed significant body weight loss (~20% of initial weight) starting around day 5, with a peak at days 7 to 9, and a slower recovery to baseline weight by day 12 to 15 (Fig. 1A). Mice inoculated with UV-inactivated hMPV did not show significant body weight loss and behaved similarly to the mock-infected control group (data not shown). Signs of illness, including ruffled fur, hunched appearance, and reduced movement, closely paralleled the curve of body weight loss (Fig. 1B). To determine hMPV replication in the lung, viral titers were assessed daily over 21 days (Fig. 1C). After an initial eclipse phase of about 1 to 2 days, viral replication could be detected in the lung starting around day 2 or 3 postinfection (p.i.), with a peak viral titer of ~10^5 $TCID_{50}$s/g of lung tissue by day 4 to 5 p.i. No replicating virus was detected in the lungs of infected mice after day 7 or 8 p.i.

BAL and lung cells, pathology, and mucus production. Compared to mock-inoculated mice, hMPV-infected mice showed a rapid increase in the number of total cells recovered from BAL fluid. In hMPV-infected mice, the number of total BAL cells increased at day 1 p.i. from $(1.5 \pm 0.7) \times 10^5$ to $(4.9 \pm 0.7) \times 10^5$, with a peak of $(8.5 \pm 0.7) \times 10^5$ at day 7 p.i. The number of BAL cells returned to near-normal values by day 21 [$(2.3 \pm 0.5) \times 10^5$] (data not shown). While the cells in BAL fluid from uninfected or mock-inoculated mice consisted mainly of macrophages, a remarkable neutrophilia was observed in hMPV-infected mice within the first 3 days (Fig. 2A). Neutrophils were still present until day 14 p.i. The numbers of mononuclear cells, including monocytes and lymphocytes, started to increase by day 3, and they represented the majority of BAL cells from day 5 to day 14 p.i. (Fig. 2A).

The lung histopathology of infected mice was compared to

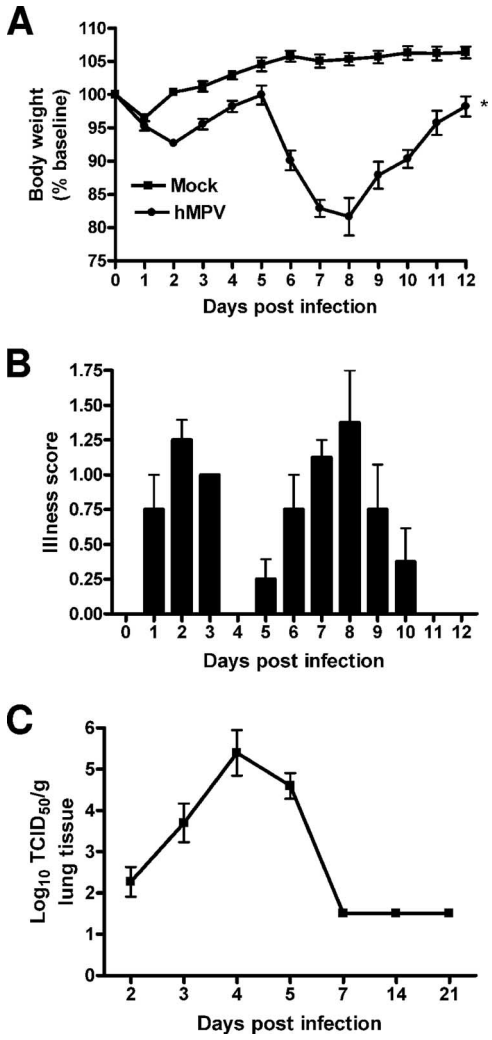

FIG. 1. hMPV-induced clinical disease and viral replication. (A) Body weight loss in hMPV-infected mice. BALB/c mice were infected i.n. with replicating hMPV at 10^7 $TCID_{50}$s. The control group received a mock inoculum. Weight is expressed as a percentage of baseline weight. Data are means ± SEM for four to six animals per group and are representative of three independent experiments. (B) Illness scores for mice infected with hMPV. Mice were assessed daily by two observers using a grading scale (from 1 to 5) as described in Materials and Methods. Data are means ± SEM for four to six mice per group. (C) hMPV replication in the lung. Infected mice were sacrificed at different days to determine viral titers by a $TCID_{50}$ assay. The lower limit of detection of this assay is 1.5 $\log_{10}$ $TCID_{50}$s/g of tissue. Data are means ± SEM (n = 4 to 6 mice/group). *, $P < 0.05$ compared to mock infection.

that of uninfected or mock-inoculated mice. Lungs of mock-inoculated mice were indistinguishable from those of uninfected mice at all time points (Fig. 2B). In hMPV-infected mice, initial changes in lung histology were noted starting at day 1 p.i., with the predominant lesion consisting of infiltration of perivascular and peribronchial areas by mononuclear cells (mainly lymphocytes and monocytes) and moderate perivascular edema. Areas with increased cellularity in alveolar septa and alveolar spaces were also present (data not shown). Pathology (expressed as the pathology score) was most severe between days 5 and 7 and was still present by day 14, although it was significantly reduced (Fig. 2B). With regard to mucus overproduction, infected mice on day 8 had increased numbers of PAS-positive cells in central and peripheral airways relative to those of control mice. These cells appeared to be hypertrophic compared with similar cells in control mice. No PAS-positive cells were seen in either the central or peripheral airways on day 1 and day 5 postinfection (Fig. 2C).

Fluorescence-activated cell sorter (FACS) analysis of lung cells showed that the numbers of $CD4^+$ and $CD8^+$ T cells increased after day 4 of infection and peaked by days 6 and 8, respectively (Fig. 3). Similarly, a peak of activated $CD4^+$ T cells (CD4/CD25) appeared to occur at day 6 p.i. The numbers of both the CD4 and CD8 T-cell subsets were still elevated 2 weeks after infection, compared to those for mock-inoculated mice. The kinetics of $Gr1^+$ neutrophil migration to the lung paralleled the kinetics observed in BAL fluid by H&E staining.

Lung function in hMPV-infected mice. When baseline lung function was measured using unrestrained whole-body plethysmography (Buxco), hMPV-infected mice consistently showed increased baseline Penh values. Penh is a dimensionless value that represents a function of the ratio of peak expiratory flow to peak inspiratory flow and a function of the timing of expiration (Fig. 4A). The increase in Penh values in hMPV-infected mice started at day 4, peaked at days 5 to 7, at the time of maximal viral replication, and subsided by day 12. Infected mice (day 14 p.i.) also had a dose-dependent increase in AHR in response to aerosolized methacholine compared to mock-inoculated mice (Fig. 4B). No significant difference in AHR, however, was recorded at earlier time points of infection (possibly due to obstruction of the airways and increased baseline Penh values). Since the accuracy of Penh as an index of airway obstruction and AHR has been a matter of scientific debate, we performed additional studies of lung mechanical properties in artificially ventilated mice. As shown in Fig. 4C, we noticed an increase in total lung respiratory resistance at baseline in hMPV-infected mice, consistent with the increased baseline Penh values observed by unrestrained plethysmography. Also in agreement with the Penh data, measurement of lung mechanics in ventilated mice confirmed that hMPV-infected mice exhibited increased airway resistance in response to inhaled methacholine starting as early as day 14 p.i., compared to uninfected controls.

Protection from reinfection. To determine whether hMPV infection resulted in protection from subsequent viral challenge, we investigated clinical illness, viral replication, and lung inflammation for mice challenged (i.e., reinfected) with hMPV (10^7 $TCID_{50}$s) 6 weeks after primary infection. Mice challenged with hMPV did not manifest the typical body weight loss observed after day 4 in primary infection (Fig. 5A) and had peak viral titers at the lower limit of detection (<1.5 $\log_{10}$ $TCID_{50}$s/g tissue) (titer in primary infection, 4.99 ± 0.05 $\log_{10}$ $TCID_{50}$s/g of tissue). Protection appeared to be virus specific, since mice infected with a related paramyxovirus, RSV, were not protected after challenge with hMPV (Fig. 5A). BAL cell counts were also significantly lower in mice challenged with hMPV than in mice with primary infections (Fig. 5B).

Serum neutralizing antibodies. Neutralizing antibody was first detectable between days 5 and 7 following hMPV infection (Fig. 6). The titer increased progressively for the next 3 weeks,

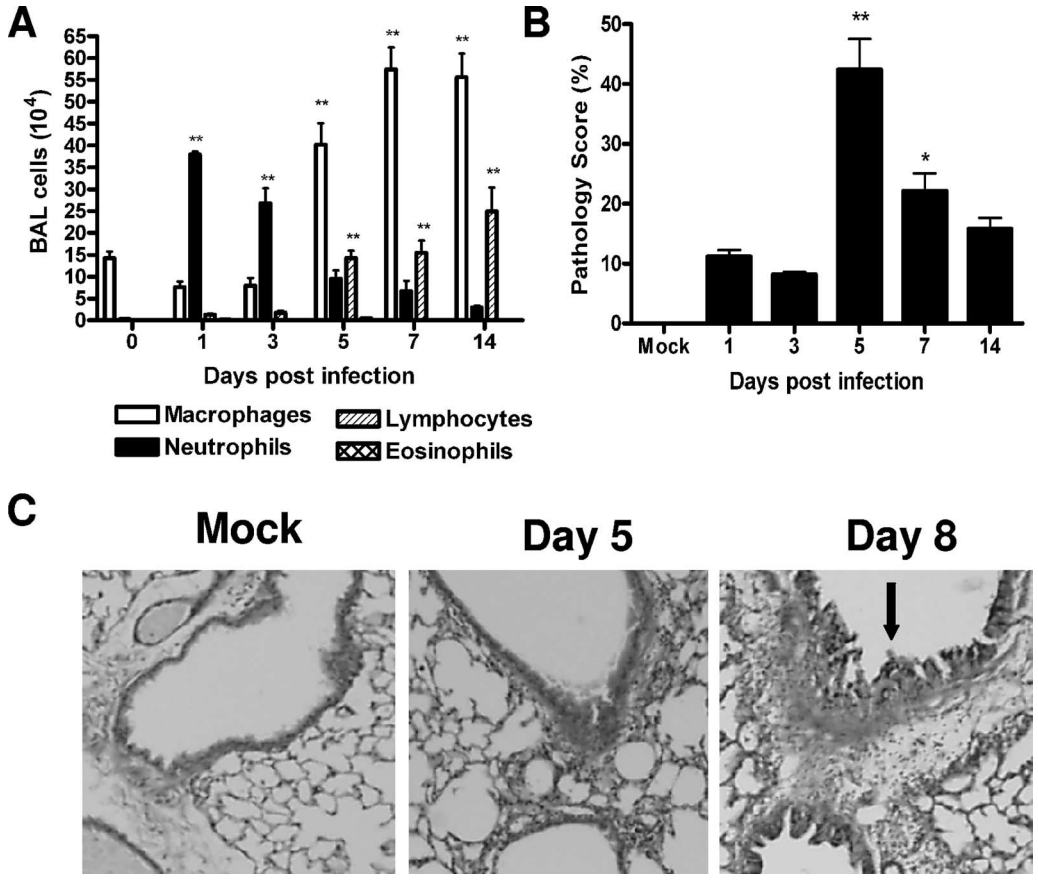

FIG. 2. Lung inflammation in hMPV-infected mice. Mice were infected with hMPV (10^7 $TCID_{50}$s) and sacrificed at day 1, 3, 5, 7, or 14. (A) Total and differential cell counts in BAL fluid from mock-inoculated and infected mice were determined. (B) Peribronchial and perivascular inflammation was assessed in lung sections stained with H&E. Data are means ± SEM for four to six mice per group. Experiments were performed in triplicate. Asterisks indicate levels of significance (*, $P < 0.05$; **, $P < 0.01$) for comparisons to mock infection. (C) Lung sections stained with PAS. Original magnification, ×40. Arrow indicates PAS-positive cells.

peaking between 4 and 6 weeks p.i., with a mean peak titer of 7.6 ± 0.4 $\log_2$. To determine whether reinfection resulted in a recall response, mice were either challenged with hMPV (10^7 $TCID_{50}$s) or sham inoculated 6 weeks after primary infection, and serum was collected 1 week p.i. for the determination of antibody titers. There was a fourfold increase in neutralizing antibody titers for mice challenged with hMPV, compared to the level of antibody present in the mice 6 weeks after primary infection (9.5 ± 0.2 $\log_2$ versus 7.6 ± 0.4 $\log_2$). There was no change in the antibody titer in previously infected mice that were sham challenged.

Role of T cells in hMPV primary infection. Previous studies with a murine model of experimental RSV infection have suggested that virus-induced illness is partially mediated by the host immune response (11). Alvarez et al. have recently reported that NK cells and T lymphocytes are necessary to control hMPV replication in the lung (1). However, the role of immune cells, specifically T lymphocytes, in the pathogenesis of hMPV-induced acute illness and in protection against reinfection has not been reported. To address these questions, BALB/c mice were depleted of either $CD4^+$ or $CD8^+$ T cells, or both, by antibodies, using two different protocols. In the first protocol, mice were treated with antibodies to deplete T-cell subsets only during the initial period of the infection (see Fig. 8A). This protocol results in depletion of both $CD4^+$ and $CD8^+$ T cells in the lung (up to 95% depletion [Fig. 7]) but has no effect on other cells, such as macrophages and dendritic cells (data not shown). As shown in Fig. 8B, mice depleted of either $CD4^+$ or $CD8^+$ T cells lost significantly less body weight than control Ig-treated or untreated mice following hMPV infection. The effect of $CD4^+$ T-cell depletion, however, was more robust than that of $CD8^+$ T-cell depletion in terms of body weight reduction. Simultaneous depletion of both T-cell subsets did not provide further protection beyond that afforded by depletion of $CD4^+$ cells alone. In agreement with the body weight loss, histopathology studies showed that depletion of $CD4^+$ cells caused a dramatic reduction in the lung pathology score, while depletion of $CD8^+$ cells was less effective (Fig. 8C). Since T lymphocytes are important for viral clearance, we assessed viral titers in the lungs of mice depleted of either $CD4^+$ or $CD8^+$ T cells, or both. Mice infected with hMPV were sacrificed at day 7 p.i., when virus is usually no longer detectable in the lung (see Fig. 1C). Mice depleted of either $CD4^+$ or $CD8^+$ T cells had detectable viral titers in the lungs, similar to those for nondepleted mice (treated with a control antibody). On the other hand, concurrent depletion of both

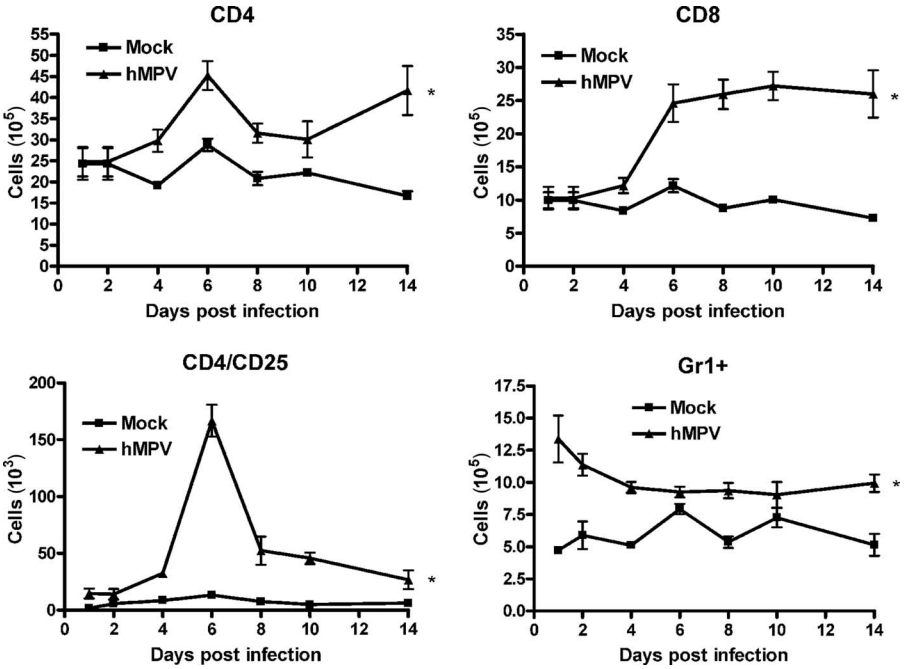

FIG. 3. FACS analysis of lung cells. Mice were either infected with hMPV or mock infected, and at different days postinfection, cells were isolated from the lung by collagenase digestion, stained with antibodies for lineage-specific markers, and analyzed by FACS. Data points are means ± SEM from five mice per group per time point and are representative of two independent experiments. *, $P < 0.05$ relative to mock infection.

T-cell subsets resulted in lung viral titers comparable to those measured at the peak of hMPV replication (Fig. 8D), indicating that both $CD4^+$ and $CD8^+$ T-cell subsets are necessary for the clearance of primary hMPV infection in the lung.

Role of T cells in hMPV reinfection. To further investigate the role of T cells in hMPV reinfection, we used a second protocol in which mice were treated with antibodies to deplete T-cell subsets until the time of viral challenge (antibodies were injected prior to and for 4 weeks following primary infection [Fig. 9A]). We first determined the effect of T-cell depletion on the generation of anti-hMPV neutralizing antibodies by measuring levels in serum prior to viral challenge. As shown in Fig. 9B, only mice depleted of $CD4^+$ T cells had undetectable serum neutralizing antibodies 4 weeks after primary viral infection. Surprisingly, we found that there was no difference among the different groups in protection against hMPV reinfection, as indicated by the absence of viral replication in the lungs of challenged mice, irrespective of depletion of T-cell subsets (Fig. 9C). Accordingly, no significant body weight loss following reinfection was observed for any of the groups, compared to mice with primary infection (Fig. 9D). These results suggest that either $CD8^+$ cells in the absence of antibody or antibody production is able to independently confer protection against a subsequent hMPV infection.

Role of T cells in hMPV-induced airway obstruction and AHR. As shown in Fig. 4A, hMPV-infected mice consistently showed increased baseline Penh values, suggesting obstruction of the airways. The increase in baseline Penh values in hMPV-infected mice started at day 4, peaked at day 5 to 7, at the time of maximal viral replication, and subsided by day 12. Acute depletion of $CD4^+$ T cells alone reduced airway obstruction at the earlier time points after infection (day 5), while depletion of $CD8^+$ T cells alone did not have a significant effect (Fig. 10A). Concurrent depletion of both $CD4^+$ and $CD8^+$ T cells had a dramatic effect on airway obstruction, with baseline Penh values that were comparable to those for mock-inoculated mice at all time points (Fig. 10A). hMPV-infected mice had slightly increased AHR in response to aerosolized methacholine challenge compared to mock-inoculated mice on day 14 and significantly increased AHR on day 21 p.i. (Fig. 10B to D; see also Fig. 4B). No significant difference in Penh was noticed at early time points of infection, probably due to obstruction of the airways and increased baseline Penh values. Concurrent depletion of $CD4^+$ and $CD8^+$ T cells completely abolished hMPV-induced AHR, while individual $CD8^+$ T-cell or $CD4^+$ T-cell depletion did not have a significant effect (Fig. 10B to D), although hMPV-infected mice depleted of the latter showed a trend to greater AHR compared to infected mice treated with a control antibody or mock-inoculated mice (Fig. 10B).

DISCUSSION

Experimental animal models for hMPV infection are needed for our understanding of pathogenesis as well as for defining immune correlates of protection. Our studies show that BALB/c mice are susceptible to hMPV, as shown by body weight loss, clinical illness scores, and viral replication (Fig. 1). Infection was characterized by an overall influx of neutrophils into the BAL fluid and lung tissue ($Gr1^+$), which was particularly evident during the first 5 days of infection. Lymphocytes were identified in the BAL fluid starting at day 3. Detailed analysis by cell-specific markers revealed an influx of both $CD4^+$ and $CD8^+$ T-cell subsets, both of which were still ele-

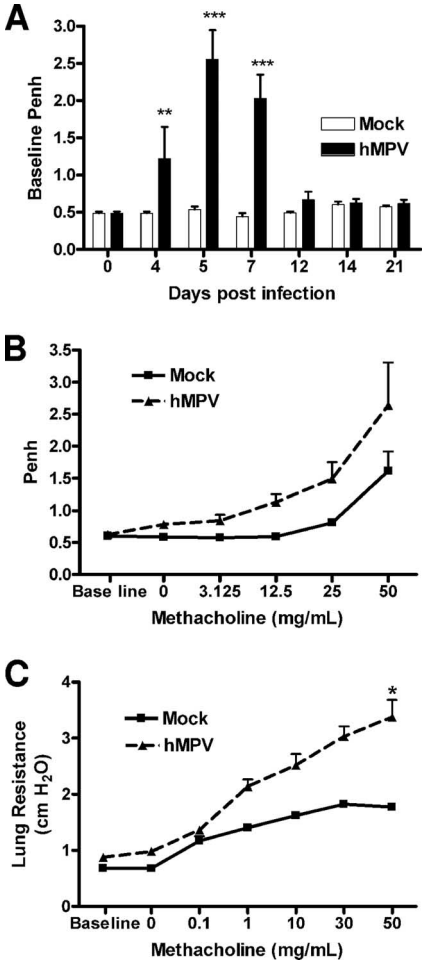

FIG. 4. Lung function in hMPV-infected mice. Mice were infected with hMPV (10^7 $TCID_{50}$s), and baseline and post-methacholine challenge Penh values were determined by unrestrained plethysmography (Buxco) for a period of 21 days. Penh is a dimensionless value that represents a function of the ratio of peak expiratory flow to peak inspiratory flow and a function of the timing of expiration. (A) Baseline Penh. (B) Penh following methacholine challenge (day 14). (C) Airway resistance (day 14) measured in mechanically ventilated mice by the Flexivent system. Data are means ± SEM for four mice per group. Asterisks indicate levels of significance (*, $P < 0.05$; **, $P < 0.01$; ***, $P < 0.001$) for comparison to mock infection.

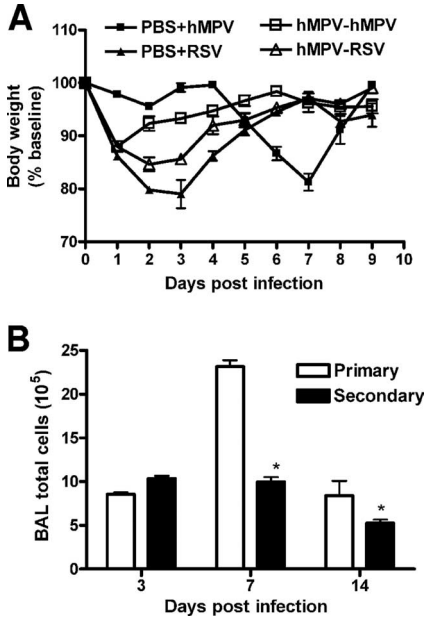

FIG. 5. Protection from reinfection. Mice were infected with hMPV (10^7 $TCID_{50}$s) and 6 weeks later were reinfected with either hMPV (10^7 $TCID_{50}$s) or RSV A2 (10^7 PFU/mouse) (A) Body weight loss after reinfection. (B) Total BAL cell counts after hMPV reinfection. Data are means ± SEM for four mice per group. *, $P < 0.05$ compared to primary infection.

vated in lung tissue 2 weeks after infection compared to levels in mock-inoculated mice. Lung histopathology was characterized by peribronchial and perivascular cell infiltration along with areas of patchy alveolitis. Maximum airway pathology was preceded by peak viral replication in the lung, while mucus overproduction was noticed first at day 8 following infection.

During infections with paramyxoviruses such as RSV, cytotoxic T lymphocytes are important for virus clearance (11, 21, 25) and play a critical role in regulating immune responses. A role for T cells in the control of replication during hMPV infection was suggested by Alvarez et al. (1), who found increased viral replication in total-T-cell-depleted mice. Our results show that mice challenged 6 weeks after primary infection with hMPV showed a lack of viral recovery from the lung along with protection from clinical disease and reduced lung inflammation. These data are consistent with previous results obtained with the murine model of RSV infection/rechallenge (10). In addition, our results show that the protective effect of primary hMPV infection against a secondary reinfection is virus specific, since the protective effect was not observed for hMPV-infected mice subsequently challenged with a related paramyxovirus (RSV).

The contribution of the T-cell-mediated immune response to hMPV clearance and disease pathogenesis was analyzed in this study for the first time. Our results clearly show that either the $CD4^+$ or the $CD8^+$ T-cell subset plays some antiviral role by itself during a primary hMPV infection, but the two subsets

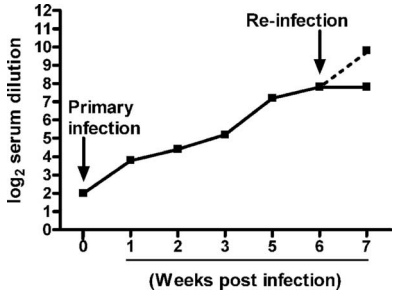

FIG. 6. Neutralizing antibodies in hMPV-infected mice. Mice were infected with hMPV (10^7 $TCID_{50}$s)and sacrificed weekly to determine antibody titers by a plaque reduction neutralization assay. The lower detection limit for this assay is 2 $\log_2$ serum dilution. At 6 weeks postinfection, mice were reinfected with hMPV, and neutralizing antibody titers were determined 1 week later. The dashed line represents titers in the sera of reinfected mice. Data are means for four to six mice per group and are representative of two experiments.

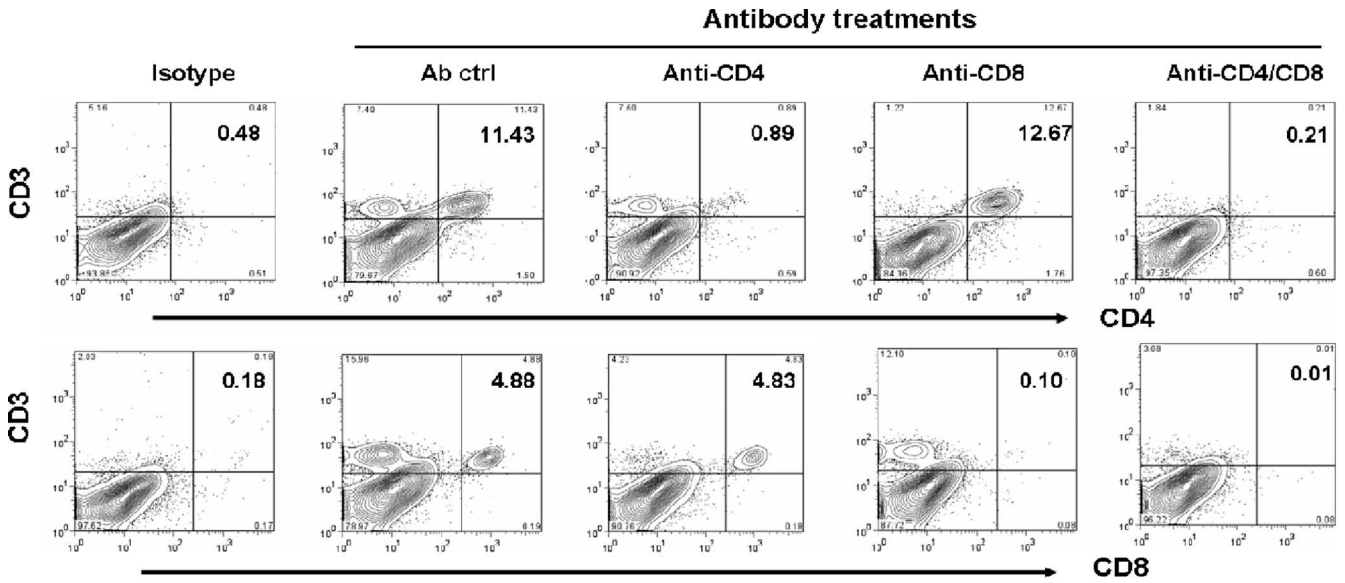

FIG. 7. Depletion of T cells from the lung. Mice were treated with anti-CD4, anti-CD8, both anti-CD4 and anti-CD8, or control antibodies (Ab ctrl), as described in Materials and Methods (protocol 1). Cells were isolated from the lung, stained with antibodies against CD3, CD4, and CD8, and analyzed by FACS. A specific reduction of >95% in the levels of CD4 and CD8 cells was observed when mice were treated with the respective antibodies alone or in combination. Isotype staining was used to set the gates for analysis of specific-antibody staining.

together can synergistically and to a much greater extent affect hMPV eradication from the lungs (Fig. 8D). Alvarez et al. (1) reported that depletion of total T cells significantly increased hMPV lung titers, suggesting that these cell types contribute to immune surveillance and control. Clinical disease, lung pathology, and early airway obstruction, on the other hand, were significantly less severe if $CD4^+$ rather than $CD8^+$ T cells were depleted (Fig. 8B and C and 10A), suggesting that primary experimental hMPV infection in mice induces a respiratory disease that is, to a large extent, immune mediated via $CD4^+$ T-cell-dependent pathways. The mechanisms that are responsible for body weight loss in hMPV-infected mice are not fully understood. It is possible that $CD4^+$ T cells, more than $CD8^+$ T cells, control the production of cytokines/mediators with cachectic activity (i.e., interleukin-6 [IL-6], tumor necrosis factor, and IL-1).

Despite the evidence that $CD4^+$ T cells were critically involved in some aspects of hMPV pathogenesis, our results also suggest that this T-cell subset may regulate other aspects of lung physiology following infection. Indeed, the trend toward increased AHR that mice developed 3 weeks after infection was exacerbated by a lack of $CD4^+$ T cells alone (Fig. 10B), yet the concurrent depletion of both $CD4^+$ and $CD8^+$ T cells completely abolished hMPV-induced airway obstruction in acute infection and AHR (Fig. 10D). The reason for these apparently opposite effects of $CD4^+$ T cells on AHR depending on whether these cells are depleted as a single-cell population or concurrently with the $CD8^+$ T-cell compartment is unclear at the moment. The trend toward increased AHR in mice lacking $CD4^+$ T cells may find an explanation in the relative shift of the T-cell populations in hMPV-infected lungs toward the $CD8^+$ T-cell compartment as a consequence of $CD4^+$ T-cell depletion. Interestingly, several recent reports have suggested that $CD8^+$ T cells are essential to the development of AHR and inflammation (20), by producing the Th2 cytokines IL-4, IL-5, and IL-13. Indeed, Alvarez and Tripp have shown that the lung T cells producing IL-4 and IL-5 at 2 to 4 weeks after hMPV infection are mainly $CD8^+$, while both $CD4^+$ and $CD8^+$ T cells produce gamma interferon (2).

The respiratory function of BALB/c mice was significantly altered by hMPV infection. Airway obstruction was present until day 8 p.i. Hamelin et al. (13) reported increased airway obstruction until day 70, whereas Darniot et al. reported that airways were obstructed only on days 1 and 2 p.i. (6). The reason for these different times for airway obstruction is unclear at the moment, but an explanation could be that these studies used different inocula and viral strains. Also, increased AHR, such as that measured by Penh in our study, has been reported previously for both RSV- and hMPV-infected mice (6, 13, 17, 26, 31). Overall, the results we obtained by unrestrained plethysmography (i.e., Penh) correlated with those obtained for mechanically ventilated mice using a Flexivent system (Fig. 4). Excess mucus production in hMPV-infected mice, as observed in our study as well as in studies by others, may be responsible in part for the airway obstruction in these mice. Although no attempt was made in this study to measure cytokines in the airways, we can speculate that the levels of IL-4, IL-5, IL-9, and IL-13 (T-cell-dependent cytokines) may be also altered in T-cell-depleted mice, and these changes, in turn, may be responsible for the changes in airway obstruction and AHR in T-cell-depleted mice following infection.

When treatment with T-cell-depleting antibodies was extended beyond the period of primary infection, the generation of serum neutralizing anti-hMPV antibodies was impaired in mice depleted of $CD4^+$ T cells but not in those depleted of $CD8^+$ T cells (Fig. 9B). Despite the lack of serum neutralizing antibodies, $CD4^+$ T-cell-depleted mice reinfected with hMPV had undetectable levels of viral replication in the lungs and

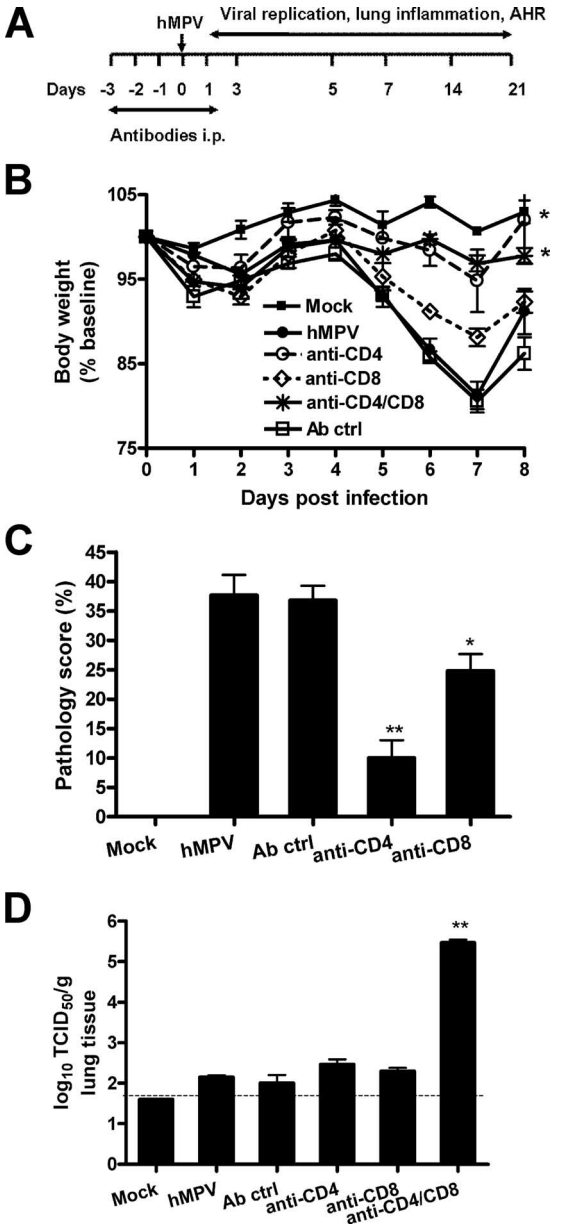

FIG. 8. Role of T lymphocytes in primary hMPV infection. Mice were treated with anti-CD4, anti-CD8, or both anti-CD4 and anti-CD8 antibodies, or with control antibodies (Ab ctrl), as described in Materials and Methods (protocol 1). Mice were either infected with hMPV or mock infected. Data are means ± SEM for four to six mice per group. Three independent experiments were performed. Asterisks indicate levels of significance (*, $P < 0.05$; **, $P < 0.01$) relative to results for hMPV-infected mice. (A) Schematic representation of the T-cell-depletion protocol. (B) Body weight loss in hMPV infection. (C) Lung peribronchial and perivascular inflammation assessed at day 7 p.i. (D) Viral replication in the lungs of BALB/c mice at day 7 p.i. by a $TCID_{50}$ assay.

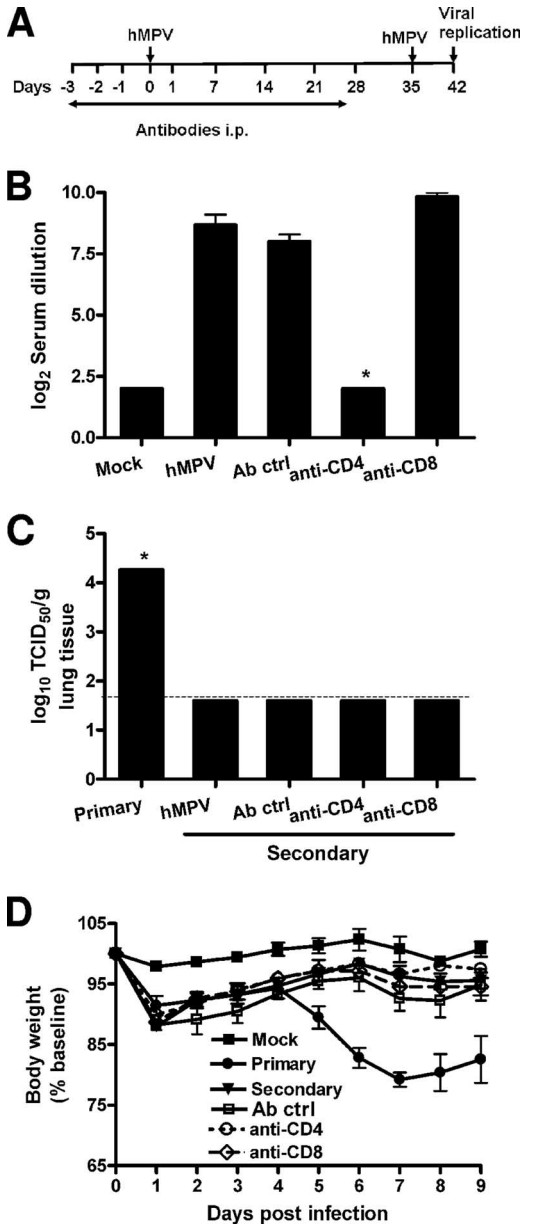

FIG. 9. Role of T lymphocytes in hMPV reinfection. Mice were treated with T-cell-depleting antibodies according to protocol 2 (see Materials and Methods) and infected with hMPV (10^7 $TCID_{50}$s). Five weeks after primary infection, mice were reinfected with the same dose of hMPV. Data are means ± SEM for four to six mice per group. Two independent experiments were performed. **, $P < 0.05$. (A) Schematic representation of the T-cell-depletion protocol. (B) Serum anti-hMPV neutralizing antibody titers were determined 4 weeks after primary infection (prior to viral challenge). (C) Viral replication in the lungs of BALB/c mice in primary and secondary infection was assessed by a $TCID_{50}$ assay. The lower limit of detection of this assay is 1.5 $\log_{10}$ $TCID_{50}$s (g of tissue)$^{-1}$. (D) Body weight loss following hMPV reinfection.

were protected from clinical disease, suggesting that, in the absence of neutralizing antibodies, protection from hMPV reinfection can be provided by an intact $CD8^+$ T-cell compartment (Fig. 9C and D). These findings are different from what has been reported previously for RSV infection of mice, in which the lack of $CD8^+$ T cells was characterized by a greater protective effect against disease than that conferred by the lack of $CD4^+$ T cells during primary infection (11). Also, mice lacking $CD4^+$ T cells and, as a consequence, lacking specific anti-RSV antibodies had significant viral replication in the lungs at the time of reinfection, while mice lacking $CD8^+$ T

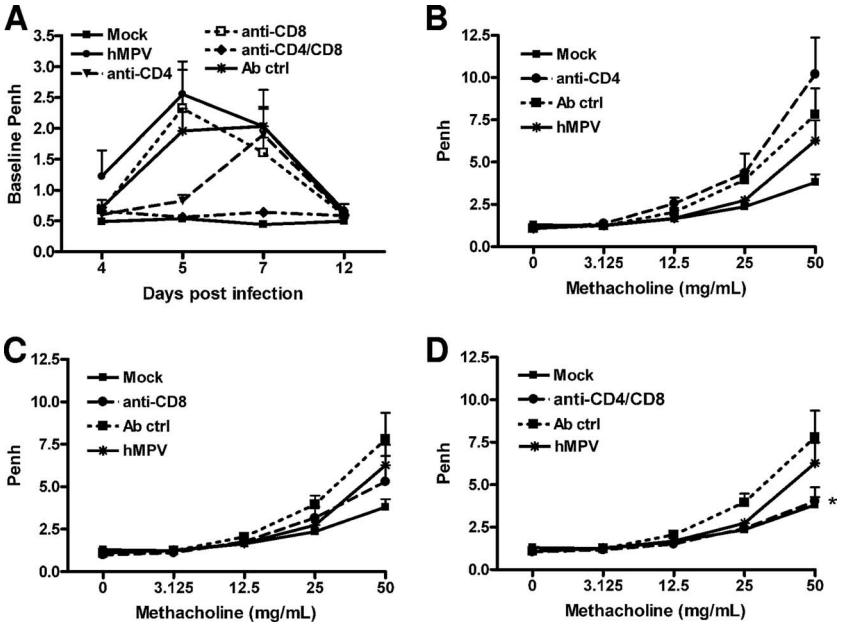

FIG. 10. Effect of T-cell depletion on lung function. Mice were treated with T-cell-depleting antibodies or control IgG (Ab ctrl), according to protocol 1 (Fig. 8A), and were infected with hMPV. Baseline Penh and post-methacholine challenge Penh (AHR) were measured for a period of 21 days following infection. (A) Baseline Penh following hMPV infection. (B through D) Effects of depletion of $CD4^+$ T cells (B), $CD8^+$ T cells (C), or both (D) on AHR (day 21). Data are means ± SEM for six mice per group. *, $P < 0.05$ compared to mock infection.

cells or immunocompetent controls had no detectable virus (11). Those $CD4^+$ T-cell-depleted mice also had more-severe clinical disease after RSV reinfection. Thus, compared to $CD4^+$ T cells, the $CD8^+$ T-cell compartment appears to be less involved in the immunopathogenesis of disease in hMPV than in RSV primary infection. In addition, the $CD8^+$ T-cell compartment appears to be sufficient to control viral replication in hMPV reinfections, while $CD4^+$ T cells (and antibodies) are clearly required for antiviral activity in the course of RSV reinfection.

While mouse models have clearly been important for understanding the immunopathogenesis of disease in the course of paramyxovirus infections, certain limitations exist when data have been extrapolated to human infections. The nature of the immune response to hMPV and its pathological features in humans are still largely unknown, and therefore our findings with mice related to the role of T cells, with regard to both their antiviral function and their contribution to clinical disease, remain to be elucidated in naturally acquired human infections.

ACKNOWLEDGMENTS

This work was supported by grants from NIAID (P01 AI062885 to A.C. and N01 AI30039 to R.P.G.) and NHLBI (N01 HV28184 to A.C. and R.P.G.) and by the Sealy Center for Vaccine Development, University of Texas Medical Branch (UTMB). D.K. was supported by the Jeane B. Kempner fellowship, UTMB.

We thank Richard Johnston for helpful suggestions on the analysis of lung mechanics.

REFERENCES

1. **Alvarez, R., K. S. Harrod, W. J. Shieh, S. Zaki, and R. A. Tripp.** 2004. Human metapneumovirus persists in BALB/c mice despite the presence of neutralizing antibodies. J. Virol. **78:**14003–14011.
2. **Alvarez, R., and R. A. Tripp.** 2005. The immune response to human metapneumovirus is associated with aberrant immunity and impaired virus clearance in BALB/c mice. J. Virol. **79:**5971–5978.
3. **Boivin, G., Y. Abed, G. Pelletier, L. Ruel, D. Moisan, S. Cote, T. C. Peret, D. D. Erdman, and L. J. Anderson.** 2002. Virological features and clinical manifestations associated with human metapneumovirus: a new paramyxovirus responsible for acute respiratory-tract infections in all age groups. J. Infect. Dis. **186:**1330–1334.
4. **Carey, M. A., J. W. Card, J. A. Bradbury, M. P. Moorman, N. Haykal-Coates, S. H. Gavett, J. P. Graves, V. R. Walker, G. P. Flake, J. W. Voltz, D. Zhu, E. R. Jacobs, A. Dakhama, G. L. Larsen, J. E. Loader, E. W. Gelfand, D. R. Germolec, K. S. Korach, and D. C. Zeldin.** 2007. Spontaneous airway hyperresponsiveness in estrogen receptor-alpha-deficient mice. Am. J. Respir. Crit. Care Med. **175:**126–135.
5. **Castro, S. M., A. Guerrero-Plata, G. Suarez-Real, P. A. Adegboyega, G. N. Colasurdo, A. M. Khan, R. P. Garofalo, and A. Casola.** 2006. Antioxidant treatment ameliorates respiratory syncytial virus-induced disease and lung inflammation. Am. J. Respir. Crit. Care Med. **174:**1361–1369.
6. **Darniot, M., T. Petrella, S. Aho, P. Pothier, and C. Manoha.** 2005. Immune response and alteration of pulmonary function after primary human metapneumovirus (hMPV) infection of BALB/c mice. Vaccine **23:**4473–4480.
7. **Esper, F., D. Boucher, C. Weibel, R. A. Martinello, and J. S. Kahn.** 2003. Human metapneumovirus infection in the United States: clinical manifestations associated with a newly emerging respiratory infection in children. Pediatrics **111:**1407–1410.
8. **Falsey, A. R., D. Erdman, L. J. Anderson, and E. E. Walsh.** 2003. Human metapneumovirus infections in young and elderly adults. J. Infect. Dis. **187:** 785–790.
9. **Freymouth, F., A. Vabret, L. Legrand, N. Eterradossi, F. Lafay-Delaire, J. Brouard, and B. Guillois.** 2003. Presence of the new human metapneumovirus in French children with bronchiolitis. Pediatr. Infect. Dis. J. **22:**92–94.
10. **Graham, B. S., L. A. Bunton, P. F. Wright, and D. T. Karzon.** 1991. Reinfection of mice with respiratory syncytial virus. J. Med. Virol. **34:**7–13.
11. **Graham, B. S., L. A. Bunton, P. F. Wright, and D. T. Karzon.** 1991. Role of T lymphocyte subsets in the pathogenesis of primary infection and rechallenge with respiratory syncytial virus in mice. J. Clin. Investig. **88:**1026–1033.
12. **Guerrero-Plata, A., S. Baron, J. S. Poast, P. A. Adegboyega, A. Casola, and R. P. Garofalo.** 2005. Activity and regulation of alpha interferon in respiratory syncytial virus and human metapneumovirus experimental infections. J. Virol. **79:**10190–10199.
13. **Hamelin, M. E., G. A. Prince, A. M. Gomez, R. Kinkead, and G. Boivin.** 2006. Human metapneumovirus infection induces long-term pulmonary inflammation associated with airway obstruction and hyperresponsiveness in mice. J. Infect. Dis. **193:**1634–1642.
14. **Hamelin, M. E., K. Yim, K. H. Kuhn, R. P. Cragin, M. Boukhvalova, J. C. Blanco, G. A. Prince, and G. Boivin.** 2005. Pathogenesis of human meta-

pneumovirus lung infection in BALB/c mice and cotton rats. J. Virol. **79:** 8894–8903.
15. **Hamelmann, E., J. Schwarze, K. Takeda, A. Oshiba, G. L. Larsen, C. G. Irvin, and E. W. Gelfand.** 1997. Noninvasive measurement of airway responsiveness in allergic mice using barometric plethysmography. Am. J. Respir. Crit. Care Med. **156:**766–775.
16. **Huck, B., D. Neumann-Haefelin, A. Schmitt-Graeff, M. Weckmann, J. Mattes, S. Ehl, and V. Falcone.** 2007. Human metapneumovirus induces more severe disease and stronger innate immune response in BALB/c mice as compared with respiratory syncytial virus. Respir. Res. **8:**6.
17. **Jafri, H. S., S. Chavez-Bueno, A. Mejias, A. M. Gomez, A. M. Rios, S. S. Nassi, M. Yusuf, P. Kapur, R. D. Hardy, J. Hatfield, B. B. Rogers, K. Krisher, and O. Ramilo.** 2004. Respiratory syncytial virus induces pneumonia, cytokine response, airway obstruction, and chronic inflammatory infiltrates associated with long-term airway hyperresponsiveness in mice. J. Infect. Dis. **189:**1856–1865.
18. **Jartti, T., B. G. van den Hoogen, R. P. Garofalo, A. D. Osterhaus, and O. Ruuskanen.** 2002. Metapneumovirus and acute wheezing in children. Lancet **360:**1393–1394.
19. **Johnston, R. A., T. A. Theman, F. L. Lu, R. D. Terry, E. S. Williams, and S. A. Shore.** 2008. Diet-induced obesity causes innate airway hyperresponsiveness to methacholine and enhances ozone-induced pulmonary inflammation. J. Appl. Physiol. **104:**1727–1735.
20. **Koya, T., N. Miyahara, K. Takeda, S. Matsubara, H. Matsuda, C. Swasey, A. Balhorn, A. Dakhama, and E. W. Gelfand.** 2007. $CD8^+$ T cell-mediated airway hyperresponsiveness and inflammation is dependent on $CD4^+$ $IL\text{-}4^+$ T cells. J. Immunol. **179:**2787–2796.
21. **Kulkarni, A. B., M. Connors, C. Y. Firestone, H. C. Morse III, and B. R. Murphy.** 1993. The cytolytic activity of pulmonary $CD8^+$ lymphocytes, induced by infection with a vaccinia virus recombinant expressing the M2 protein of respiratory syncytial virus (RSV), correlates with resistance to RSV infection in mice. J. Virol. **67:**1044–1049.
22. **MacPhail, M., J. H. Schickli, R. S. Tang, J. Kaur, C. Robinson, R. A. Fouchier, A. D. Osterhaus, R. R. Spaete, and A. A. Haller.** 2004. Identification of small-animal and primate models for evaluation of vaccine candidates for human metapneumovirus (hMPV) and implications for hMPV vaccine design. J. Gen. Virol. **85:**1655–1663.
23. **Milligan, G. N., D. I. Bernstein, and N. Bourne.** 1998. T lymphocytes are required for protection of the vaginal mucosae and sensory ganglia of immune mice against reinfection with herpes simplex virus type 2. J. Immunol. **160:**6093–6100.
24. **Nissen, M. D., D. J. Siebert, I. M. Mackay, T. P. Sloots, and S. J. Withers.** 2002. Evidence of human metapneumovirus in Australian children. Med. J. Aust. **176:**188.
25. **Rutigliano, J. A., M. T. Rock, A. K. Johnson, J. E. Crowe, Jr., and B. S. Graham.** 2005. Identification of an $H\text{-}2D^b$-restricted $CD8^+$ cytotoxic T lymphocyte epitope in the matrix protein of respiratory syncytial virus. Virology **337:**335–343.
26. **Schwarze, J., G. Cieslewicz, E. Hamelmann, A. Joetham, L. D. Shultz, M. C. Lamers, and E. W. Gelfand.** 1999. IL-5 and eosinophils are essential for the development of airway hyperresponsiveness following acute respiratory syncytial virus infection. J. Immunol. **162:**2997–3004.
27. **Schwarze, J., E. Hamelmann, K. L. Bradley, K. Takeda, and E. W. Gelfand.** 1997. Respiratory syncytial virus infection results in airway hyperresponsiveness and enhanced airway sensitization to allergen. J. Clin. Investig. **100:** 226–233.
28. **Stockton, J., I. Stephenson, D. Fleming, and M. Zambon.** 2002. Human metapneumovirus as a cause of community-acquired respiratory illness. Emerg. Infect. Dis. **8:**897–901.
29. **van den Hoogen, B. G., T. M. Bestebroer, A. D. Osterhaus, and R. A. Fouchier.** 2002. Analysis of the genomic sequence of a human metapneumovirus. Virology **295:**119–132.
30. **van den Hoogen, B. G., J. C. de Jong, J. Groen, T. Kuiken, R. de Groot, R. A. Fouchier, and A. D. Osterhaus.** 2001. A newly discovered human pneumovirus isolated from young children with respiratory tract disease. Nat. Med. **7:**719–724.
31. **van Schaik, S. M., G. Enhorning, I. Vargas, and R. C. Welliver.** 1998. Respiratory syncytial virus affects pulmonary function in BALB/c mice. J. Infect. Dis. **177:**269–276.
32. **Williams, J. V., P. A. Harris, S. J. Tollefson, L. L. Halburnt-Rush, J. M. Pingsterhaus, K. M. Edwards, P. F. Wright, and J. E. Crowe, Jr.** 2004. Human metapneumovirus and lower respiratory tract disease in otherwise healthy infants and children. N. Engl. J. Med. **350:**443–450.
33. **Williams, J. V., S. J. Tollefson, J. E. Johnson, and J. E. Crowe, Jr.** 2005. The cotton rat (*Sigmodon hispidus*) is a permissive small animal model of human metapneumovirus infection, pathogenesis, and protective immunity. J. Virol. **79:**10944–10951.
34. **Wyde, P. R., S. N. Chetty, A. M. Jewell, S. L. Schoonover, and P. A. Piedra.** 2005. Development of a cotton rat-human metapneumovirus (hMPV) model for identifying and evaluating potential hMPV antivirals and vaccines. Antivir. Res. **66:**57–66.